Available online www.jocpr.com

Journal of Chemical and Pharmaceutical Research, 2017, 9(7):40-54

Research Article

ISSN : 0975-7384
CODEN(USA) : JCPRC5

Electrochemical Determination of Dopamine, Uric acid and Ascorbic acid at $Mn_{0.02}Sn_{0.98}O_2$ Nanoparticles Modified Carbon Paste Electrode

MP Deepak[1*], MP Rajeeva[2] and GP Mamatha[2]

[1]*Department of Pharmaceutical Chemistry, Kuvempu University, Karnataka, India*
[2]*Department of Physics, Kuvempu University, Jnana Sahyadri, Karnataka, India*

ABSTRACT

The synthesis of $Mn_{0.02}Sn_{0.98}O_2$ nanoparticles by gel combustion method. These synthesized $Mn_{0.02}Sn_{0.980}O_2$ nanoparticles were characterised by XRD and SEM. $Mn_{0.02}Sn_{0.980}O_2$ nanoparticles modified carbon paste electrode (MSNMCPE) was developed by known procedure. The surface morphology of MSNMCPE was confirmed by SEM. The determination of dopamine (DA), uric acid (UA) and ascorbic acid (AA) has been studied at MSNMCPE by cyclic voltammetric technique. The MSNMCPE showed very good sensitivity for DA, UA and AA compare to bare CPE. The results suggest that the nature of electrode reaction was diffusion controlled. The low detection limit (LOD) and low quantification limit (LOQ) of DA, UA, AA were detected. The preparation of the modified electrode was easy, renewed by simple polishing gives very good reproducibility, high stability in its voltammetric response and low detection limit for DA, UA and AA.

Keywords: Dopamine; Uric acid; Ascorbic acid; $Mn_{0.02}Sn_{0.98}O_2$ nanoparticles; Cyclic voltammetry

INTRODUCTION

In recent years the designing, fabrication and application of novel electrochemical sensor has been of considerable interest [1]. A major problem in DA determination is the resolution between DA and coexisting species such as uric acid (UA) and ascorbic acid (AA). UA is a primary product of purine metabolism in the human body [2]. Its abnormal concentration level causes many diseases, such as gout, hyperuricaemia and Lesch-Nyan disease [3]. Therefore, the research of UA determination is of great importance in reality [4]. AA is a water soluble vitamin, and is a compound that takes part in many important life processes. It is one of the most important vitamins, due to its antioxidant and pH regulator properties often being added to various food products and pharmaceuticals [5]. UA and AA are both present in biological fluids such as blood and urine [6]. As reported, the concentration of AA is generally much higher than that of DA (100 to 1000 times) [7]. At traditional electrodes, UA and AA are oxidized at potentials close to that of DA, resulting in an overlapping voltammetric response [8-10]. The regenerated DA returns to the electrode, resulting in an enhanced current [11]. A variety of examples of the electrochemical determination of DA and UA along with AA have been proposed. These include a carbon paste electrode using zinc oxide nanoparticles and a new ferrocene-derivative modified carbon paste electrode [12], voltammetric sensor employing $CuFe_2O_4$ nanoparticles and room temperature ionic liquids [13], A novel modified carbon paste electrode based on NiO/CNTs nanocomposite and (9, 10-dihydro-9, 10-ethanoanthracene-11, 12-dicarboximido)-4-ethylbenzene-1, 2-diol as a mediator [14], FePt/CNTs nanocomposite/*N*-(4-hydroxyphenyl)-3,5-dinitrobenzamide modified carbon paste electrode [15], Modified multiwall carbon nanotubes modified electrode [16], Ethynylferrocene–NiO/MWCNT nanocomposite modified carbon paste electrode [17], ZnO/CNT nanocomposite room temperature ionic liquid modified carbon paste electrode [18], Poly (L-Tyrosine)/SnO_2 nanoparticles modified carbon paste electrode [19]. $Ni_{0.02}Sn_{0.98}O_2$ nanoparticles modified carbon paste electrode [20]. In this work carbon paste electrode is modified with $Mn_{0.02}Sn_{0.98}O_2$ nanoparticles and applied for the electrochemical investigation for dopamine, uric acid, Ascorbic acid.

EXPERIMENTAL SECTION

Reagent and Chemicals

Tin (II) chloride dehydrate ($SnCl_2.H_2O$, 99.99%, Merck), Nitric acid (HNO_3, 70%, Merck), Manganese Chloride Hexahydrate ($MgCl_2.6H_2O$), Citric acid ($C_6H_8O_7$, 99.5%, Merck), Potassium ferrocyanide $K_4[Fe(CN)_6]$, DA, AA and UA solutions were prepared by dissolving in double distilled water. DA was prepared by dissolving in 0.1 M per chloric acid ($HClO_4$) solution, 0.1 M potassium chloride (KCl) was used as supporting electrolyte for all analytes.

Apparatus and Procedure

The electrochemical experiments were carried out by using an Electroanalyser model EA-201 chemlink system. The instrumentation involves three-electrode system. The electrode system contained a carbon paste electrode as working electrode, saturated calomel electrode as reference electrode and platinum wire as counter electrode. $Mn_{0.02}Sn_{0.98}O_2$ nanoparticles modified carbon paste electrode was prepared by grinding the 10mg of $Mn_{0.02}Sn_{0.98}O_2$ nanoparticles with 70% graphite powder and 30% silicon oil in an agate mortar by hand mixing for about 30 minute to get homogenous $Mn_{0.02}Sn_{0.98}O_2$ nanoparticles modified carbon paste electrode. The paste was packed into the cavity of CPE and smoothened on weighing paper. The bare CPE was prepared without adding modifier.

Synthesis of $Mn_{0.02}Sn_{0.98}O_2$ Nanoparticles by Gel Combustion Method

In synthesis used materials were tin (II) chloride dehydrate, 6.2 mole of nitric acid was an oxidizer and mixed in an appropriate ratio to form a tin nitrate solution, to this solution 1.5 mole of citric acid which acts as fuel and 0.02 mL Manganese chloride Hexahydrate were added and then heated at 90°C in a Pyrex vessel with constant stirring. When the temperature was incresed to about 300°C, a polymeric precursor underwent a strong, self-sustaining combustion reaction occurs with evolution of large volume of gases and swelled into voluminous and foamy ashes. The entire combustion process held in a few seconds. The produced ashes were then calcined about 800°C (for 1 hour). This process was carried out until the complete decomposition of carbonaceous residues. Finally white powder $Mn_{0.02}Sn_{0.98}O_2$ nanoparticles were obtained [21].

RESULTS AND DISCUSSION

Characterization of Synthesized $Mn_{0.02}Sn_{0.98}O_2$ Nanoparticles by XRD and SEM

Crystallite size and Crystalline structure of $Mn_{0.02}Sn_{0.98}O_2$ nanoparticles were analyzed by Cu-K_α X-ray radiation (λ=1.5418A°) in 2θ range from 20° to 80° operating at 30 kV and 15 mA. The scan rate was 5°/min.). XRD patterns as shown in Figure 1, the average grain size was calculated using the Scherrer relation,

$$d = 0.89\frac{\lambda}{\beta\cos\theta} \quad \ldots\ldots\ldots\ldots\ldots\ldots\ldots\ldots\ldots\ldots\ldots (1)$$

Where d is the crystallite size, λ is the wavelength of X-rays, β is the full width of half maximum and 2θ is the diffraction peak angle [22],

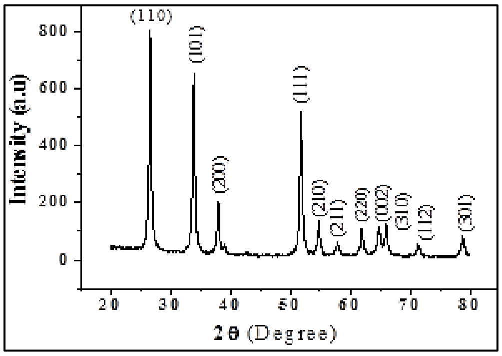

Figure 1: XRD images of synthesized of $Mn_{0.02}Sn_{0.98}O_2$ nanoparticles

The crystallite sizes of $Mn_{0.02}Sn_{0.98}O_2$ nanoparticles were found to be 23.03 nm by using Scherrer formula. The surface morphology of the nanoparticles of powdered samples was investigated by scanning electron microscope

(SEM) (Hitachi Model S-3200N). Figure 2 shows the typical SEM image synthesized of the $Mn_{0.02}Sn_{0.98}O_2$ nanoparticles.

SEM Characterization of $Mn_{0.02}Sn_{0.98}O_2$ Nanoparticles Modified Carbon Paste Electrode (MSNMCPE)

The morphology of the CPE and MSNMCPE were characterized by scanning electron microscope (SEM) as shown in Figures 3a and 3b respectively. Smooth surface was observed on bare CPE surface. While modified electrode the formation of spindle-like nanostructures not only enlarges the surface area of the electrode and also improves the electron transfer rate between the electrode surface and the bulk solution, which has been confirmed by the performance of MSNMCPE in electrochemical investigation of $K_4[Fe(CN)_6]$ system.

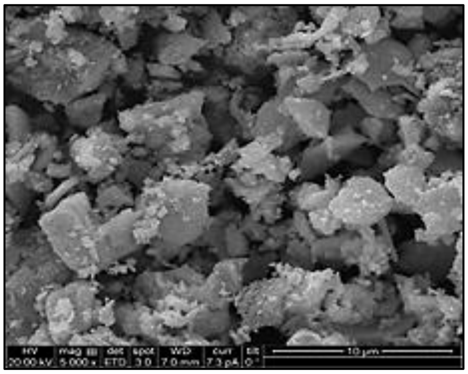

Figure 2: SEM images of synthesized $Mn_{0.02}Sn_{0.98}O_2$ nanoparticles

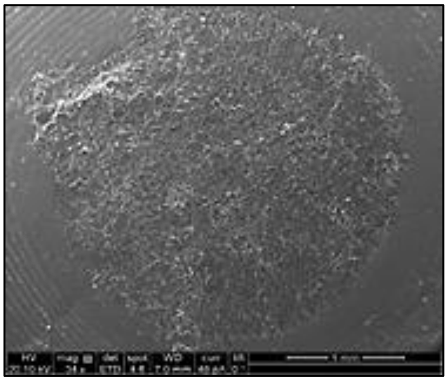

Figure 3a: SEM image of bare carbon paste electrode

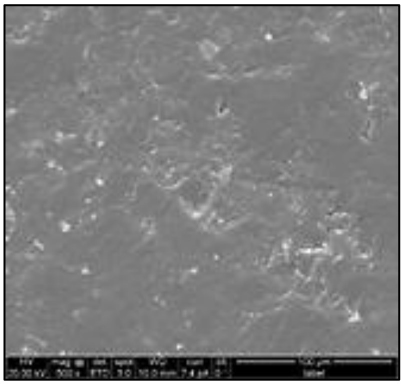

Figure 3b: SEM image of $Mn_{0.02}Sn_{0.98}O_2$ nanoparticles modified carbon paste electrode

Electrochemical Response of $K_4[Fe(CN)_6]$ at $Mn_{0.02}Sn_{0.98}O_2$ Nanoparticles Modified Carbon Paste Electrode

In Figure 4 shows the electrochemical investigation of 1 mM potassium ferrocyanide ($K_4[Fe(CN)_6]$) in 1M KCl at bare carbon paste electrode (BCPE) represented as curve 'b' and at $Mn_{0.02}Sn_{0.98}O_2$ nanoparticles modified carbon paste electrode (MSNMCPE) represented as curve 'a' respectively. The curve 'b' indicates the E_{pc} 240 mV of cathodic peak current I_{pc} 5.56 µA and E_{pa} 403 mV of anodic peak current I_{pa} 6.24 µA at BCPE. Whereas, for the

MSNMCPE the E_{pc} 253 mV of cathodic peak current I_{pc} 12.61 µA E_{pa} 334 mV and of anodic peak current I_{pa} 18.61 µA has been observed. The excellent peak current enhancement showed at MSNMCPE. The surface area of bare CPE was 0.027 cm^2, whereas effective surface area of the modified electrode was found to be 0.036 cm^2.

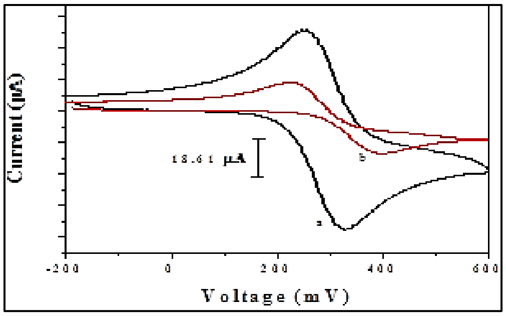

Figure 4: Comparision of 0.1 mM K4[Fe(CN)6] in 0.1 M KCl solution at $Mn_{0.02}Sn_{0.98}O_2$ nanoparticles modified carbon paste electrode (a) and bare carbon paste electrode (b)

Electrochemical Investigation of Dopamine (DA) at $Mn_{0.02}Sn_{0.98}O_2$ Nanoparticles Modified Carbon Paste Electrode (MSNMCPE)

The electrochemical investigation of 0.1 mM dopamine in 0.1 M phosphate buffer solution of pH 7 has been studied at MSNMCPE using cyclic voltammetric technique. In Figure 5 represents the cyclic voltammograms of 0.1 mM DA at bare CPE (curve 'b') and at MSNMCPE (curve 'a'). The curve 'c' shows the cyclic voltammogram of blank solution at MSNMCPE. Which confirms the modification of bare CPE, above studies showed that redox behavior of DA. The peak potentials E_{pa} and E_{pc} were found to be 272 and 80 mV with peak current I_{pa} and I_{pc} of 2.05 µA and 0.9 µA respectively at bare CPE, whereas peak potentials E_{pa} and E_{pc} were found to be 257 mV and at 101 mV with peak currents I_{pa} 5.63 µA and I_{pc} 2.27 µA at respectively at MSNMCPE in the potential range from -200 to 600 mV. The peak was observed in the reverse scan, suggesting that the electrochemical reaction is a totally quasireversible process and the redox peak at the bare CPE is broad due to slow electron transfer, while the response was considerably improved at MSNMCPE and the peaks potentials shifted to negative direction, the shape of the peaks turns sharper and the peak current increased significantly.

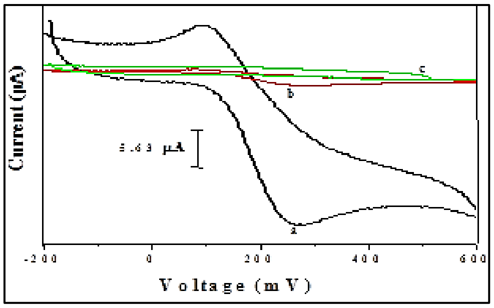

Figure 5: Comparision of 0.1 mM DA at $Mn_{0.02}Sn_{0.98}O_2$ nanoparticles modified carbon paste electrode (a), bare carbon paste electrode (b) and blank solution in 0.1 M phosphate buffer at $Mn_{0.02}Sn_{0.98}O_2$ nanoparticles modified carbon paste electrode (c); pH 7, scan rate 25 mVs^{-1}

Electrochemical Investigation of Uric Acid (UA) at $Mn_{0.02}Sn_{0.98}O_2$ Nanoparticles Modified Carbon Paste Electrode

In Figure 6 shows cyclic voltammograms of 0.1 mM UA at bare carbon paste electrode (BCPE) (curve 'b') and at MSNMCPE (curve 'a'). The curve 'c' represents the cyclic voltammogram of blank solution at MSNMCPE, which confirms the modification of bare CPE. Here only one oxidation peak current of 1.12 µA at with 442 mV at bare CPE, whereas an oxidation peak current of 4.69 µA with 384 mV at MSNMCPE in the potential range from 100 to 600 mV. No reduction peak was observed in the reverse scan suggesting that the electrochemical reaction is a totally irreversible proce.

Electrochemical Investigation of Ascorbic Acid (AA) at $Mn_{0.02}Sn_{0.98}O_2$ Nanoparticles Modified Carbon Paste Electrode

The Ascorbic acid (AA) was behavior in 0.1 M phosphate buffer solution of pH 5.5 at MSNMCPE using cyclic voltammetric technique. Figure 7 shows cyclic voltammograms of 0.1 mM AA at bare CPE (curve 'b') and at MSNMCPE (curve 'a') also at MSNMCPE in blank solution (curve 'c'), which shows the conformation of modification of bare CPE. Above studies showed that only one oxidation peak potential at 412 mV with peak current of 5.12 µA at bare CPE, whereas an oxidation peak potential at 334 mV with peak current of 28.55 µA at MSNMCPE in the potential range from -200 to 600 mV. No reduction peak was observed in the reverse scan, suggesting that the electrochemical reaction is a totally irreversible process and the oxidation peak current at MSNMCPE.

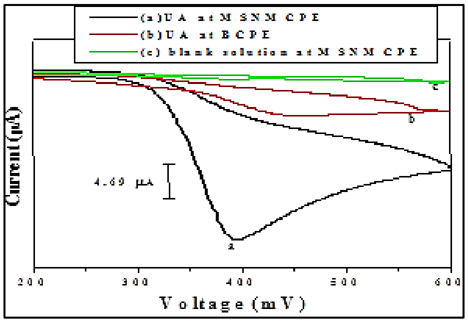

Figure 6: Comparision of 0.1 mM UA at $Mn_{0.02}Sn_{0.98}O_2$ nanoparticles modified carbon paste electrode (a), bare carbon paste electrode (b) and blank solution in phosphate buffer solution at $Mn_{0.02}Sn_{0.98}O_2$ nanoparticles modified carbon paste electrode (c); pH 6.5, scan rate 10 mVs^{-1}

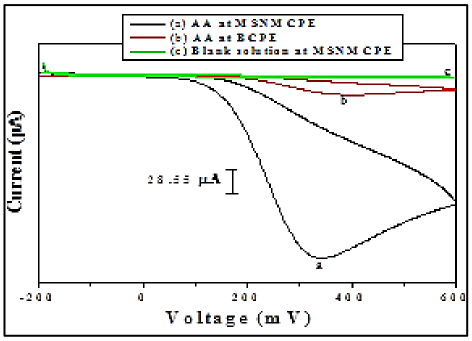

Figure 7: Comparision of 1 mM AA at $Mn_{0.02}Sn_{0.98}O_2$ nanoparticles modified carbon paste electrode (a), bare carbon paste electrode (b) and blank solution in 0.1 M phosphate bufferat $Mn_{0.02}Sn_{0.98}O_2$ nanoparticles modified carbon paste electrode (c); pH 5.5, scan rate 10 mVs^{-1}

Effect of pH on DA, UA and AA

The electrooxidation of DA was studied at 0.1 mM stock solution over pH range from 4 to 9 using 0.1 M phosphate buffer solution (PBS) of scan rate 50 mVs^{-1} at MSNMCPE by cyclic voltammetric technique. The oxidation peak current increases with increase of pH from 4 to 7 and becomes maximum and peak potential shifted negatively. While pH beyond 7, a great decrease of the anodic peak current could be observed, then it decreased gradually with the further increase in pH of the solution is shown in Figure 7a and the anodic peak potential decreases with increase in pH of the solution shown in Figure 7b. The corresponding linear regression equation is

$$E_{pa}(mV) = 829.436 - 74.836pH\ (R = 0.99687)\ldots\ldots\ldots\ldots\ldots\ldots\ldots\ (2)$$

The value of this slope is in close agreement with the theoretical value of 59 mV/pH at 25° for a $2e^-$ transfer process. Other researchers also have reported $2e^-$ transfer oxidation process in DA [23,24]. The effect of pH on UA has been studied by using the 0.1 mM stock solution of UA in 0.1 M PBS in the pH range from 2.5 to 9 of a scan rate 50 mVs^{-1} at MSNMCPE using cyclic voltammetric technique. The anodic peak current decreases with increase of pH from 2.5 to 6.5 and becomes maximum and peak potential shifted negatively at pH 6.5. While pH beyond 6.5, a great decrease of the oxidation peak current could be observed, then it decreased gradually with the further increase in the pH of solution is shown in Figure 8a and the oxidation peak potential decrease with increase in the pH as shown in Figure 8b.The corresponding linear regression equation is

$$E_{pa}(mV) = 670.47 - 38.052pH\ R = 0.9582\ldots\ldots\ldots\ldots\ldots\ldots\ldots\ (3)$$

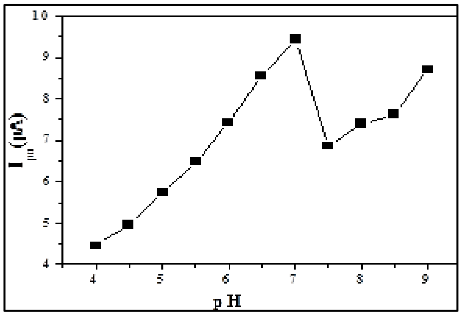

Figure 7a: Plot of anodic peak current vs. pH (4 – 9) of 0.1 mM DA at $Mn_{0.02}Sn_{0.98}O_2$ nanoparticles modified carbon paste electrode

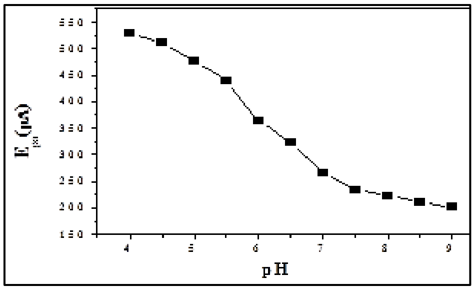

Figure 7b: Plot of anodic peak potential vs. pH (4-9) of 0.1 mM DA at$Mn_{0.02}Sn_{0.98}O_2$ nanoparticles modified carbon paste electrode

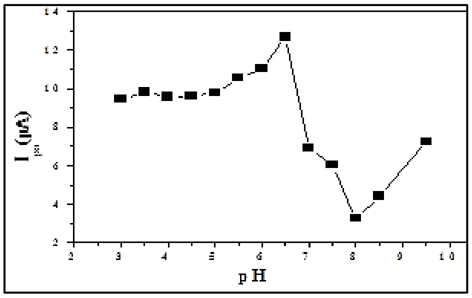

Figure 8a: Plot of anodic peak current vs. pH (3–9.5) of 0.1 mM UA at Mn0.02Sn0.98O2 nanoparticles modified carbon paste electrode

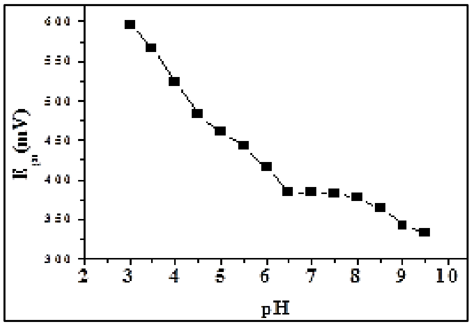

Figure 8b: Plot of anodic peak potential vs. pH (3–9.5) of 0.1 mM UA at $Mn_{0.02}Sn_{0.98}O_2$ nanoparticles modified carbon paste electrode

The negative slope of 38.640 was close to the theoretical value indicated that the electrons and protons involved in the oxidation of UA were equal (1:1). Similarly, the effect of pH on electro oxidation of AA of 0.1 mM stock solution in 0.1 M PBS in pH range from 3 to 9 of a scan rate 50 mVs^{-1} at MSNMCPE using cyclic voltammetric technique has been studied. The anodic peak current decreases with increase of pH from 3 to 5.5 and becomes maximum and peak potential shifted negatively at pH 5.5. While pH beyond 5.5, a great decrease of the oxidation peak current could be observed, then it decreased gradually with the further increasing the pH of solution is shown in Figure 9a and the oxidation peak potential decrease with increase in the pH is shown in Figure 9b the relationship between the anodic peak potential and pH is explained with the following equation.

$$E_{pa}(mV) = 521.10 - 31.04pH \quad R = 0.9050 \ldots\ldots\ldots\ldots (4)$$

The negative slope of 31.04 was close to the theoretical value indicated that the electrons and protons involved in the oxidation of AA.

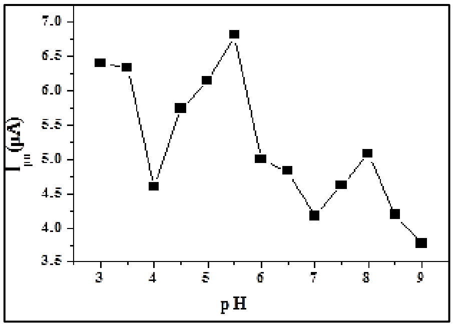

Figure 9a: Plot of anodic peak current vs. pH (3-9) of 0.1 mM AA at $Mn_{0.02}Sn_{0.98}O_2$ nanoparticles modified carbon paste electrode

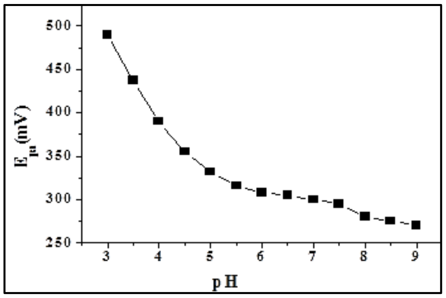

Figure 9b: Plot of anodic peak potential vs. pH (3-9) of 0.1 mM AA at $Mn_{0.02}Sn_{0.98}O_2$ nanoparticles modified carbon paste electrode

Effect of scan rate on DA, UA and AA

The effect of scan rates on the electrochemical response of 0.1 mM DA at MSNMCPE was studied at different scan rates were 25, 50, 75, 100, 125, 150, 175, 200 mVs^{-1} by CV and the cyclic voltammograms as shown in Figure 10a.

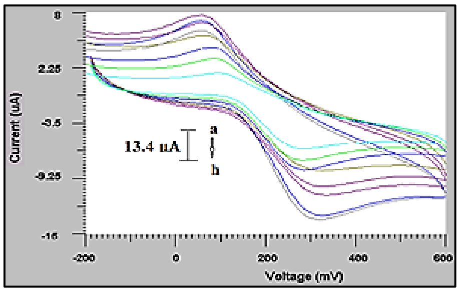

Figure 10a: Cyclic voltammogram of 0.1 mM DA at $Mn_{0.02}Sn_{0.98}O_2$ nanoparticles modified carbon paste electrode with different scan rates (a) 25, (b) 50, (c) 75, (d) 100, (e) 125, (f) 150, (g) 175, (h) 200 mVs^{-1}

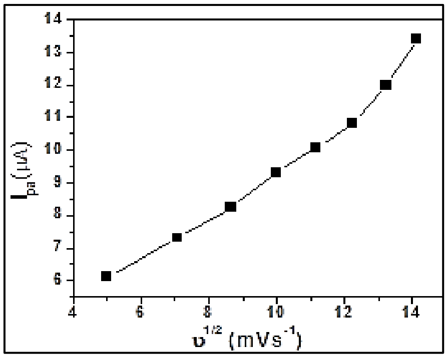

Figure 10b: Plot of anodic peak current vs. square root of scan rates of DA at $Mn_{0.02}Sn_{0.98}O_2$ nanoparticles modified carbon paste electrode

The Figure 10b shows the linear relationship between the peak current and square root of scan rate with a correlation coefficient of 0.9977 obtained between the anodic peak current and square root of scan rate in the range of 25 – 200 mVs^{-1}. The corresponding linear regression equation is

$I_{pa}(\mu A) = 0.7624\nu^{1/2} + 1.8863$ R = 0.9862…………………………… (5)

which revealed that a diffusion controlled process at MSNMCPE. However linearity was also obtained for the plot of anodic peak current vs. the scan rate with a correlation coefficient of 0.9903 shown in Figure 10c and the corresponding linear regression equation was given by:

$I_{pa}(\mu A) = 0.03952\nu + 5.2103$ R = 0.99692…………………………... (6)

The results suggest that the nature of electrode reaction was diffusion controlled and as a result the peak potential shifts towards positive side.

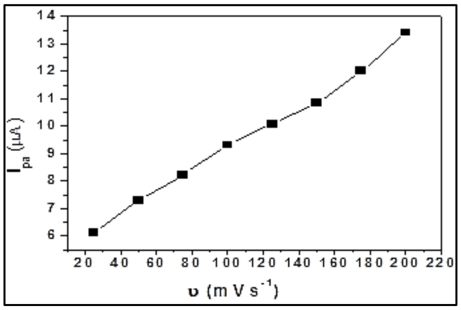

Figure 10c: Plot of anodic peak current vs. scan rates of DA at $Mn_{0.02}Sn_{0.98}O_2$ nanoparticles modified carbon paste electrode

The relationship between the anodic peak potential and scan rate is explained by plotting of the anodic peak potential vs. natural logarithm scan rate Figure 10d by considering the relation:

$E_{pa}(mV) = 0.02830 \ln \upsilon + 0.1132$ R= 0.9978……………………….. (7)

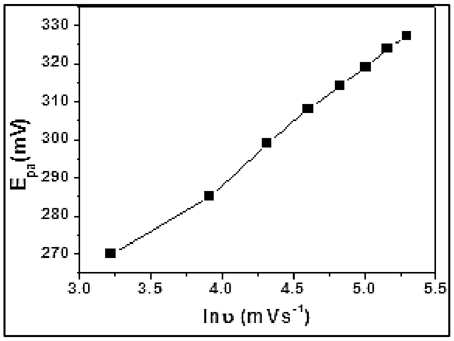

Figure 10d: Plot of anodic peak potential vs. natural logarithm of scan rates of DA at $Mn_{0.02}Sn_{0.98}O_2$ nanoparticles modified carbon paste electrode

To study the effect of scan rate on UA, 0.1 mM UA in 0.1 M PBS was studied for different scan rates from 10 to 150 mVs^{-1}at MSNMCPE by CV and the cyclic voltammograms were shown in Figure 11a.

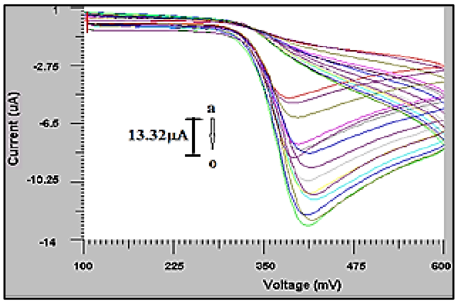

Figure 11a: Cyclic voltammograms of 0.1 mM UA at $Mn_{0.02}Sn_{0.98}O_2$ nanoparticles modified carbon paste electrode with different scan rates (a) 10, (b) 20, (c) 30, (d) 40, (e) 50, (f) 60, (g) 70, (h) 80, (i) 90, (j) 100 (k) 110 (l) 120 (m) 130 (n) 140 (o) 150 mVs^{-1}

The Figure 11b shows linear relationship between peak current and square root of scan rate with a correlation coefficient of 0.9959 obtained between anodic peak current and square root of scan rate in the range of 10 – 150 mVs^{-1}. The corresponding linear regression equation is

I_{pa} (μA) = $0.9864ν^{1/2} + 0.7314$ R = 0.9960…………………….. (8)

which revealed that a diffusion controlled process occurring at MSNMCPE.

The linearity was also obtained for the plot of anodic peak current of vs. scan rate with a correlation coefficient of 0.9953 shown in Figure 11c.

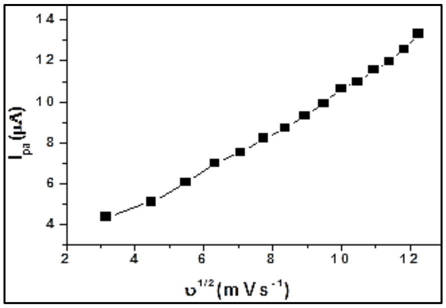

Figure 11b: Plot of anodic peak current vs. square root of scan rates of UA at $Mn_{0.02}Sn_{0.98}O_2$ nanoparticles modified carbon paste electrode

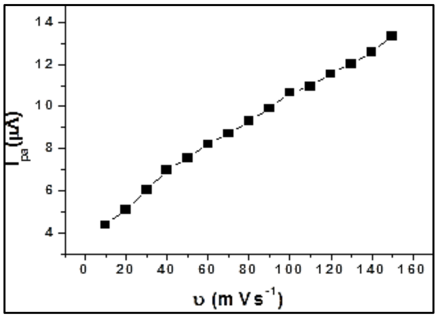

Figure 11c: Plot of anodic peak current vs. scan rates of UA at $Mn_{0.02}Sn_{0.98}O_2$ nanoparticles modified carbon paste electrode

The relationship between the anodic peak potential and scan rate is explained by plotting of the anodic peak potentials vs. natural logarithm of scan rate Figure 11d by considering the relation:

E_{pa}(mV) = 0.0166lnυ + 0.3360, R = 0.9915………………… (9)

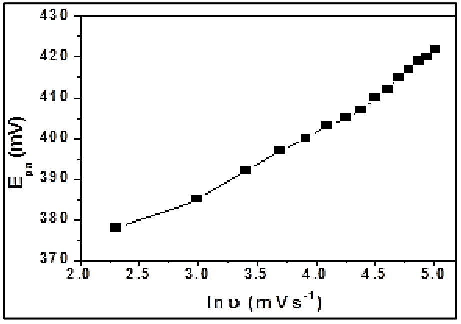

Figure 11d: Plot of anodic peak potential vs. natural logarithm of scan rates of UA at $Mn_{0.02}Sn_{0.98}O_2$ nanoparticles modified carbon paste electrode

The linear relation between logI_{pa} and logν Figure 11e is corresponding to the following equation

logI_{pa} (μA) = 0.425logν- 0.1713 (R = 0.9919)………………. (10)

The slope for the equation is 0.425, which is close to the theoretical value of 0.5 for a diffusion controlled process between scan rates 10 - 150 mVs^{-1}.

Similarly, the effect of scan rate on 0.1 mM AA for different scan rates 10, 20, 30, 40, 50, 60 70, 80, 90 and 100 mVs^{-1} at MSNMCPE has been studied by CV and the corresponding cyclic voltammograms were shown in Figure 12a.

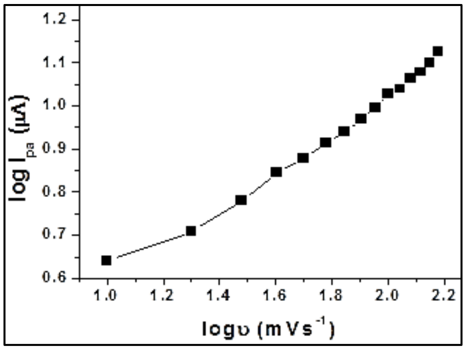

Figure 11e: Plot of logarithm of anodic peak potential vs. logarithm of scan rates of UA at $Mn_{0.02}Sn_{0.98}O_2$ nanoparticles modified carbon paste electrode

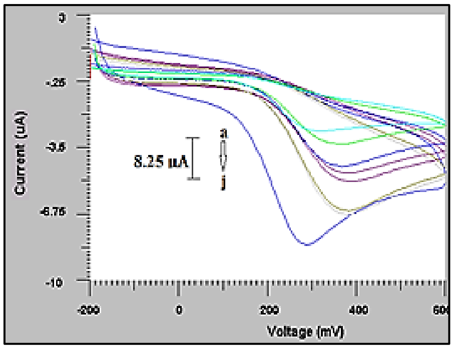

Figure 12a: Cyclic voltammograms of 0.1 mM AA at $Mn_{0.02}Sn_{0.98}O_2$ nanoparticles modified carbon paste electrode with different scan rates (a) 10, (b) 20, (c) 30, (d) 40, (e) 50, (f) 60, (g) 70, (h) 80, (i) 90, (j) 100 mVs^{-1}

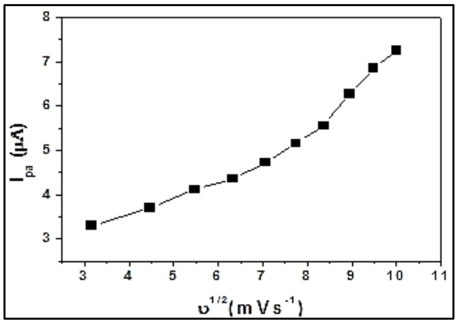

Figure 12b: Plot of anodic peak current vs. square root of scan rates of AA at $Mn_{0.02}Sn_{0.98}O_2$ nanoparticles modified carbon paste electrode

The Figure 12b shows the linear relationship between the peak current and square root of scan rate with a correlation coefficient of 0.9959 obtained between the anodic peak current and square root of scan rate in the range of 10 – 100 mVs^{-1}.The corresponding linear regression equation is

I_{pa} (μA) = $0.9864\nu^{1/2} + 0.7314$ R = 0.99608……………… (11)

Which revealed that a diffusion controlled process occurring at the MSNMCPE. The linearity was also obtained for the plot of scan rate vs. the anodic peak current with a correlation coefficient of 0.9953 shown in Figure 12c.

The relationship between the anodic peak potential and scan rate was revealed by plotting of anodic peak potentials vs. natural logarithm of scan rate Figure 12d by considering the relation:

E_{pa} (mV) = 0.0166 lnυ + 0.3360 R = 0.9915………………….. (12)

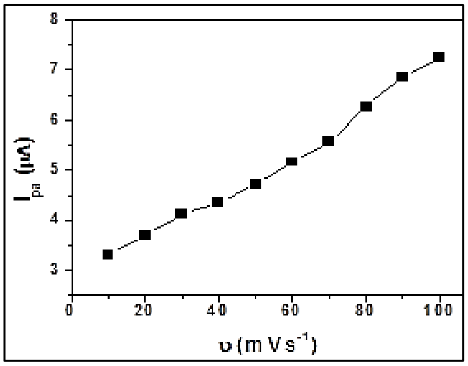

Figure 12c: Plot of anodic peak current vs. scan rates of AA at $Mn_{0.02}Sn_{0.98}O_2$ nanoparticles modified carbon paste electrode

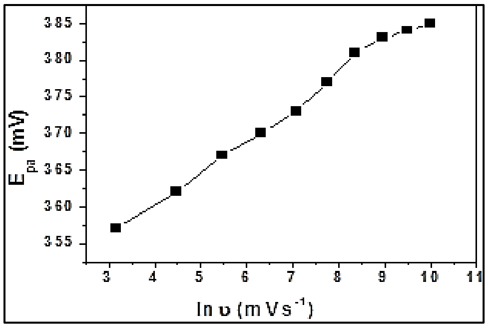

Figure 12d: Plot of anodic peak potential vs. natural logarithm of scan rates of AA at $Mn_{0.02}Sn_{0.98}O_2$ nanoparticles modified carbon paste electrode

According to Laviron's theory [25], the slope is equal to $RT/\alpha n_\alpha F$. The value of αn_α was found to 0.4542. As for a totally quasi-reversible electrode reaction process of dopamine and irreversible electrode reaction process of uric acid and ascorbic acid respectively. The n_α was calculated as 1.73, 2.4708 and 1.709 respectively, which indicated that two electrons were involved in the oxidation process of dopamine, uric acid and ascorbic acid at MSNMCPE. Since the equal number of electron and proton took part in the oxidation of dopamine, uric acid and ascorbic acid therefore two electrons and two protons transfer were involved in the electrode reaction process. The electrochemical reaction process for dopamine, uric acid and ascorbic acid at MSNMCPE is summarized in Scheme 1.

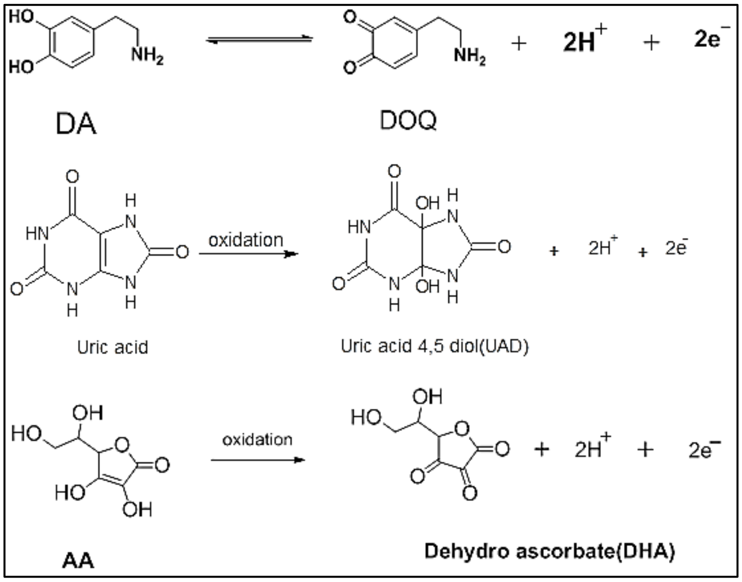

Scheme 1: Probable oxidation of DA, UA and AA

Calibration of Dopamine, Uric acid and Ascorbic Acid Concentration:

A series of dopamine, uric acid and ascorbic acid solutions of range1.0×10^{-5} to 1.0×10^{-3} M were prepared in PBS to investigate the relationship between the anodic peak current (I_{pa}) and concentration of dopamine, uric acid and ascorbic acid at $Mn_{0.02}Sn_{0.98}O_2$ nanoparticles modified carbon paste electrode at a scan rate of 25, 10 and 10 mVs^{-1} by cyclic voltammetry. The obtained cyclic voltammograms of DA, UA and AA were shown in Figures 13a-13c respectively.

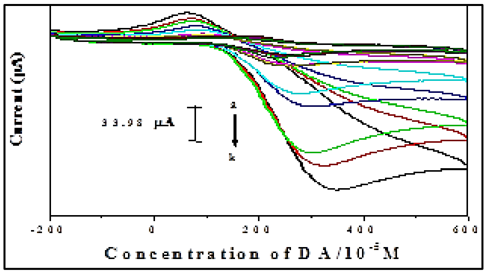

Figure 13a: Effect of variation of concentration of DA (a) 1×10^{-5} M, (b) 2×10^{-5} M,(c) 4×10^{-5} M, (d) 6×10^{-5} M, (e) 8×10^{-5} M, (f) 1×10^{-4} M, (g) 2×10^{-4} M, (h) 4×10^{-4}M(i) 6×10^{-4}M, (j) 8×10^{-4} M,(k) 1×10^{-3} M on anodic peak current at $Mn_{0.02}Sn_{0.98}O_2$ nanoparticles modified carbon paste electrode; scan rate 25 mVs^{-1}

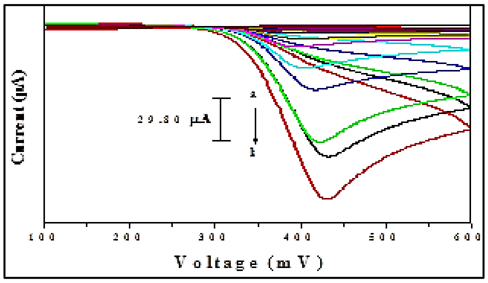

Figure 13b: Effect of variation of concentration of UA (a) 1×10^{-5} M, (b) 2×10^{-5} M, (c) 4×10^{-5} M, (d) 6×10^{-5} M, (e) 8×10^{-5} M, (f) 1×10^{-4} M,(g) 2×10^{-4}M, (h) 4×10^{-4} M, (i) 6×10^{-4}M, (j) 8×10^{-4}M,(k) 1×10^{-3} M on anodic peak current at $Mn_{0.02}Sn_{0.98}O_2$ nanoparticles modified carbon paste electrode; scan rate 10 mVs^{-1}

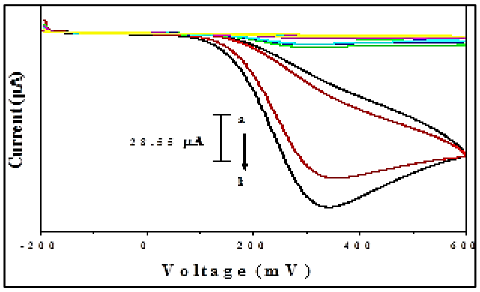

Figure 13c: Effect of variation of concentration of AA (a) 1×10^{-5} M, (b) 2×10^{-5} M, (c) 4×10^{-5} M,(d) 6×10^{-5} M, (e) 8×10^{-5} M, (f) 1×10^{-4} M,(g) 2×10^{-4} M, (h) 4×10^{-4}M (i) 6×10^{-4}M, (j) 8×10^{-4}M (k) 1×10^{-3} M on anodic peak current at $Mn_{0.02}Sn_{0.98}O_2$ nanoparticles modified carbon paste electrode; scan rate 10 mVs^{-1}

A linear relationship has obtained on plotting I_{pa} versus concentration of DA, UA and AA which is shown in Figures 14a-14c respectively, this is explained on the basis of linear regression equations for DA, UA and AA respectively were expressed as:

I_{pa} (µA) = 32.341C (10^{-5} M) + 2.0089 R= 0.9930………………… (13)

I_{pa} (µA) = 38.505C (10^{-5} M) + 0.5114 R= 0.9970……………….... (14)

I_{pa} (µA) = 29.239C (10^{-5} M) + 0.0497 R= 0.9970………………… (15)

The limit of detection (LOD) and limit of quantification (LOQ) were 1.316 µM, 4.389 µM for DA, 0.848 µM, 2.82 µM for UA and 0.965 µM, 3.216 µM for AA.

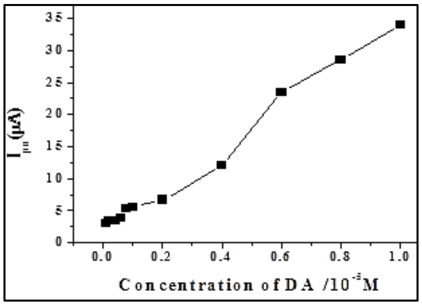

Figure 14a: Plot of anodic peak current vs. concentration of DA at $Mn_{0.02}Sn_{0.98}O_2$ nanoparticles modified carbon paste electrode

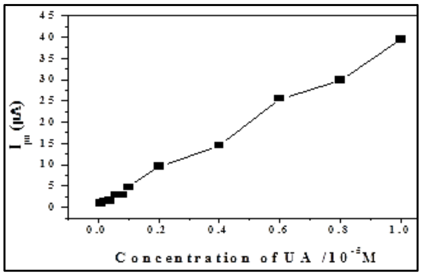

Figure 14b: Plot of anodic peak current vs. concentration of UA at $Mn_{0.02}Sn_{0.98}O_2$ nanoparticles modified carbon paste electrode

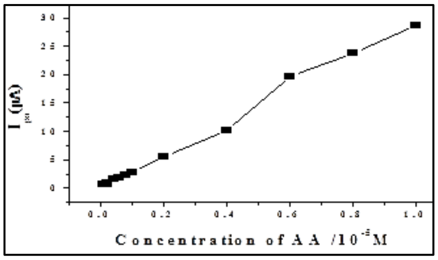

Figure 14c: Plot of anodic peak current vs. concentration of AA at $Mn_{0.02}Sn_{0.98}O_2$ nanoparticles modified carbon paste electrode

The LOD and LOQ were calculated on the peak current using the following equation:
LOD= 3S/M, LOQ=10S/M
Where, S is standard deviation and M is the slope of calibration plot.

Simultaneous Determination of DA, UA and UA, AA at $Mn_{0.02}Sn_{0.98}O_2$ Nanoparticles Modified Carbon Paste Electrode by Cyclic Voltammetry

Simultaneous determination of DA, UA and AA, UA in 0.1 M PBS of pH 7 and pH 5.5 carried at bare and MSNMCPE. The corresponding cyclic voltammograms as showed in Figures 15a and 15b respectively. In the Figure 15a the curve 'b' exhibits one broad peak for the solution containing 0.5 mM DA and 0.2 mM UA mixture at bare CPE, which indicates that the bare CPE fails to separate the voltammetric signals of DA and UA. Whereas the curve 'a' exhibits two well defined oxidation peaks at potentials at 272 and 354 mV for 0.5mM DA and 0.2 mM UA at modified carbon paste electrode indicating the efficiency of the modified electrode. Thus MSNMCPE can be effectively employed to separate DA and UA. Similarly in Figure 15b the curve 'b' exhibits one broad peak for the solution containing 1 mM AA and 0.2 mM UA mixture at bare CPE. The curve 'a' exhibits two oxidation peaks at potentials 367 and 486 mV for AA and UA respectively at modified carbon paste electrode indicating the efficiency of modified electrode in separating the voltammetric signals AA and UA respectively. Thus MSNMCPE can be effectively employed to separate DA, UA and AA, UA.

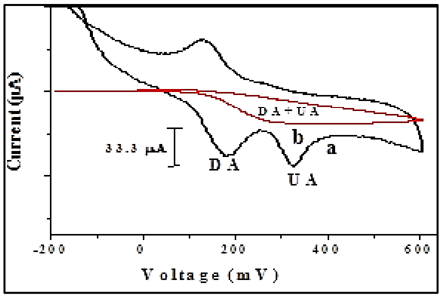

Figure 15a: Cyclic voltammograms at $Mn_{0.02}Sn_{0.98}O_2$ nanoparticles modified carbon paste electrode (a) and bare carbon paste electrode (b) in presence of 0.5 mM DA and 0.2 mM UA in 0.1 M PBS of pH 7; scan rate 25 mVs^{-1}

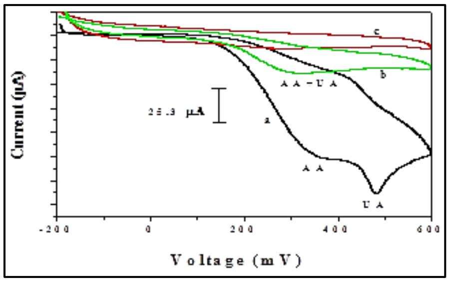

Figure 15b: Cyclic voltammograms at $Mn_{0.02}Sn_{0.98}O_2$ nanoparticles modified carbon paste electrode (a), bare carbon paste electrode (b) in presence of 1 mM AA and 0.2 mM UA and blank solution in0.1 M PBS at $Mn_{0.02}Sn_{0.98}O_2$ nanoparticles modified carbon paste electrode; pH 5.5, scan rate 10 mVs^{-1}

Resolution of DA, UA and AA, UA by Differential Pulse Voltammetry (DPV)

Differential pulse voltammetry (DPV) was used to investigate the possibility of MSNMCPE for simultaneous determination of DA, UA and AA, UA. The modified electrode separates DA, UA and AA, UA mixture. As the concentration of mixture increases, current also increases which shown in Figures 16a and 16b.

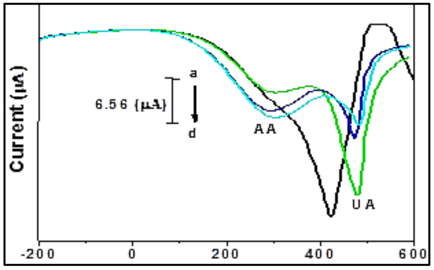

Figure 16a: Differential pulse voltammograms of AA and UA at $Mn_{0.02}Sn_{0.98}O_2$ nanoparticles modified carbon paste electrodeat pH 5.5 in PBS with scan rate 10 mVs^{-1}. (a) 0.5 mM UA + 0.2 (a), 0.4 (b), 0.6 (c) and 0.8 mM AA(d)

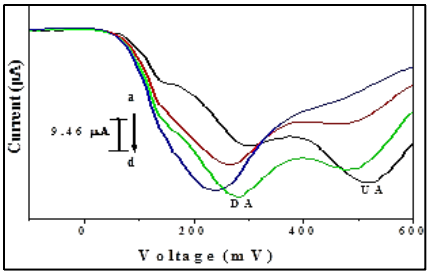

Figure 16b: Differential pulse voltammograms of DA and UA at $Mn_{0.02}Sn_{0.98}O_2$ nanoparticles modified carbon paste electrodein pH 7.0 PBS with the scan rate 25 mVs^{-1}, 0.5 mM DA + 0.1 (a), 0.2 (b), 0.3 (c) and 0.4 mM UA(d)

Simultaneous determination of DA, UA and AA by differential pulse voltammetry (DPV)\

Figure 17 shows the differential pulse voltammograms of mixed solution of 0.5 mM DA, 0.2 mM UA and 1mM AA of pH 5.5. The curve shows three oxidation peaks at potentials 492, 524, 279 mV for AA, DA and UA respectively. This suggests that the MSNMCPE can be effectively employed to separate DA, UA and AA.

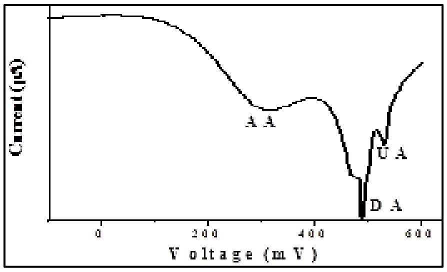

Figure 17: Differential pulse voltammograms of 0.2 mM AA and 0.5 mM DA in presence of 1mM UA at $Mn_{0.02}Sn_{0.98}O_2$ nanoparticles modified carbon paste electrode with scan rate 25 mVs^{-1}

CONCLUSION

In this work, $Mn_{0.02}Sn_{0.98}O_2$ nanoparticles modified CPE was fabricated and the characteristics of the electrode is studied. The present work has indicated that $Mn_{0.02}Sn_{0.98}O_2$ nanoparticles modified carbon paste electrode improved the electrochemical activities towards the oxidation of DA, UA and AA. Large peak separation allows the modified electrode for the simultaneous determination of DA, UA in the PBS of pH 7.0 and AA, UA in PBS of pH 5.5 by CV and DPV techniques. Linear calibration plots for the oxidation of DA, UA and AA were obtained in the range of 1×10^{-5} M to 1×10^{-3} M.

The detection limits (LOD) of DA, UA and AA at $Mn_{0.02}Sn_{0.98}O_2$ nanoparticles modified carbon paste electrodewere found to be 1.316, 0.848, 0.965 µM respectively. The proposed method has been practically and successfully applied for the simultaneous determination of DA, UA and AA. Due to its good stability and reproducibility the $Mn_{0.02}Sn_{0.98}O_2$ nanoparticles modifiedcarbon paste electrode can be used for the simultaneous measurement of DA, UA and AA.

REFERENCE

[1] RM Wightman; LJ May; AC Michael. *Anal Chem*. **1988**, 60, 769A.
[2] J Premkumar; SB Khoo. *J Electroana Chem.* **2005** 576, 105.
[3] CR Raj; F Kitamura; T Ohsaka. *Analyst.* **2002**, 9, 1155.
[4] Lin Mei Niu; Hong DunLoud; Nian Bing Li. *Inst Sci Technol.* **2007**, 35, 59.
[5] JB Raoof; Ojani; A Kiani. *J Electroanal Chem.* **2001**, 515, 45.
[6] Zhongua Wang; Yiming Wang; Guoan Luo. *Analyst.* **2002**, 127, 1353.
[7] RM Wightman; LJ May; AC Michael. *Anal Chem.* **1988**, 60, 769A.
[8] F Gonon; M Buda; R Cespuglio; M Jouvet; JF Pujol. *Nature.* **1980**, 286, 902.
[9] RD O'Neill. *Analyst.* **1994**, 119, 767.
[10] A Salimi; H Mam-Khezri; R Hallaj. *Talanta.* **2006**, 70, 823.
[11] MA Dayton; AG Ewing; RM Wightman. *Anal Chem.* **1980**, 52, 2392.
[12] H Karimi-Maleh; K Ahanjan; M Taghavi; M Ghaemy. *Anal Methods*. **2016**, 8, 1780-1788.
[13] R Bavandpour; H Karimi-Maleh; M Asif; VK Gupta; N Atar; M Abbasghorban. *J Mol Liq*. **2016**, 213, 369-373.
[14] H Karimi-Maleh; P Biparva and M Hatami. *Biosens Bioelectron*. **2013**, 48, 270-275.
[15] H Karimi-Maleh; F Tahernejad-Javazmi; AA Ensafi; R Moradi; S Mallakpour; H Beitollahi. *Biosens Bioelectron*. **2014**, 60, 1-7.
[16] AA Ensafi; H Karimi-Maleh. *J Electroanalytical Chem*. **2010**, 640, 75-83.
[17] MR Shahmiri; Ali Bahari; H Karimi-Maleh; R Hosseinzadeh; N Mirnia. *Sensors Actuators B Chem*. **2013**, 177, 70-77.
[18] E Afsharmanesh; H Karimi-Maleh; A Pahlavan; J Vahedi. *J Mol Liq*. **2013**, 181, 8-13.
[19] MP Deepak; GP Mamatha. *Anal Bioanal Electrochem*. **2015**, 7, 523-538.
[20] MPDeepak; MP Rajeeva; GP Mamatha. *Anal Bioanal Electrochem*. **2016**, 8, 931-947.
[21] MP Rajeeva; CS Naveen; Ashok R Leman; HS Jayanna. *AIP Conf Proc*. **2013**, 183, 1536.
[22] L Patterson. *Phys Rev Online Arch.* **1939**, 56, 978.
[23] QG Von Nehring; JW Hightower; JL Anderson. *Anal Chem.* **1986**, 58, 2777.
[24] MP Siswana; KI Ozoemena; T Nyokong. *Electrochem Acta.* **2006**, 52 114.
[25] EJ Laviron. *Electroanal Chem*. **1974**, 52, 355.